Static and dynamic alterations in the amplitude of low-frequency fluctuation in patients with amyotrophic lateral sclerosis

Xujing Ma[1], Fengmei Lu[2,3], Heng Chen[4], Caihong Hu[1], Jiao Wang[1], Sheng Zhang[1], Shuqin Zhang[1], Guiran Yang[1] *, Jiuquan Zhang[5,6,7,8] *

[1] Department of Medical Technology, Cangzhou Medical College, Cangzhou, China.

[2] The Clinical Hospital of Chengdu Brain Science Institute, Chengdu, China.

[3] MOE Key Lab for Neuroinformation, School of life Science and technology, University of Electronic Science and Technology of China, Chengdu, China.

[4] School of medicine, Guizhou University, Guiyang, China.

[5] Department of Radiology, Chongqing University Cancer Hospital, Chongqing, China

[6] Key Laboratory for Biorheological Science and Technology of Ministry of Education, Chongqing University, Chongqing, China.

[7] Chongqing Cancer Institute, Chongqing, China.

[8] Chongqing Cancer Hospital, Chongqing, China.

Corresponding Author:

Jiuquan Zhang

Chongqing 400030, PR China.

Email address: zhangjq_radiol@foxmail.com.

And

Guiran Yang

Cangzhou 061001, PR China.

E-mail: yangguiran2006@126.com.

Abstract

Background: Static changes in local brain activity in patients suffering from amyotrophic lateral sclerosis (ALS) have been studied. However, the dynamic characteristics of local brain activity are poorly understood. Whether dynamic alterations could differentiate patients with ALS from healthy controls (HCs) remains unclear.

Methods: A total of 54 patients with ALS (mean age = 48.71 years, male/female = 36/18) and 54 (mean age = 48.30 years, male/female = 36/18) HCs underwent magnetic resonance imaging scans. To depict static alterations in cortical activity, amplitude of low-frequency fluctuations (ALFF) which measures the total power of regional activity was computed. Dynamic ALFF (d-ALFF) from all subjects was calculated using a sliding-window approach. Statistical differences in ALFF and d-ALFF between both groups were used as features to explore whether they could differentiate ALS from HC through support vector machine method.

Results: In contrast with HCs, patients with ALS displayed increased ALFF in the right inferior temporal gyrus and bilateral frontal gyrus and decreased ALFF in the left middle occipital gyrus and left precentral gyrus. Furthermore, patients with ALS demonstrated lower d-ALFF in widespread regions, including the right lingual gyrus, left superior temporal gyrus, bilateral precentral gyrus, and left paracentral lobule by comparison with HCs. Furthermore, the ALFF in the left superior orbitofrontal gyrus had a tendency of correlation with ALSFRS-R score and disease progression rate. The classification performance in distinguishing ALS was higher with both features of ALFF and d-ALFF than that with a single approach.

Conclusions: Decreased dynamic brain activity in the precentral gyrus, paracentral gyrus, lingual gyrus, and temporal regions was found in ALS group. The combined ALFF and d-ALFF could distinguish ALS from HCs with a higher accuracy than ALFF and d-ALFF alone. These findings may provide important evidence for understanding the neuropathology underlying ALS.

Introduction

Amyotrophic lateral sclerosis (ALS) is a devastating disease which involves dysfunctions in movement and cognition (Hardiman et al. 2017; van Es et al. 2017). Patients with ALS usually died within 3–5 years after symptoms appear (Roth & Shacka 2009). At present, the therapeutic options for ALS are limited. Nevertheless, increasing lines of evidence demonstrate that early diagnosis is important for selecting available pharmacologic therapy and that appropriate palliative care has an active influence on patients' living quality and survival (Bourke et al. 2006;

61   Volanti et al. 2011). Now the diagnosis of ALS is still clinical, and a pronounced delay exists

62   between the onset of symptoms and diagnosis, possibly beyond the therapeutic window (Turner

63   et al. 2009). Timely and accurate diagnosis of ALS is urgently needed to date, and imaging

64   biomarkers should be developed.

65   Recent studies combining functional and structural data depicted that functional alterations

66   at resting state may precede structural changes in patients with cognitive impairments (Kawagoe

67   et al. 2019; Sun et al. 2016) and ALS (Abidi et al. 2020; Chipika et al. 2019). Neuroimaging

68   approaches provide convenience for studying local brain activities and may facilitate expanding

69   our understanding of early diagnosis of ALS (Huynh et al. 2016; Verstraete & Foerster 2015).

70   Resting-state functional magnetic resonance imaging (rs-fMRI) is an ideal instrument used to

71   probe into cortical activities based on blood oxygenation level-dependent signals without

72   performing variable tasks (Biswal et al. 1995). As an effective index to measure local brain

73   activity, amplitude of low frequency fluctuation (ALFF) (Guo et al. 2012; Liu et al. 2013; Yu-

74   Feng et al. 2007) has been extensively employed in ALS research. Using this approach, scholars

75   have discovered that patients with ALS showed aberrant activation in the precentral gyrus,

76   frontal gyrus, and occipital regions; this finding suggests that ALS is a disease involving many

77   system with brain impairment spreading beyond the motor cortex (Bueno et al. 2019; Ma et al.

78   2016; Shen et al. 2018). In addition, the increased ALFF in the frontal lobe could be a candidate

79   biomarker in ALS (Luo et al. 2012). However, these studies are on the strength of the hypothesis

80   that the signal of rs-fMRI is static during scanning, ignoring the dynamic behavior of activities of

81   people's brains (Allen et al. 2014; Fu et al. 2017; Liu et al. 2017).

82   Dynamic amplitude of low-frequency fluctuation (d-ALFF), an indicator of the variance of

83   ALFF, is an effective tool to explore brain dynamics in healthy people (Liao et al. 2019; Zou et

84   al. 2009) and patients with neuropsychiatric disorders, including schizophrenia (Yang et al.

85   2019), generalized anxiety disorder (GAD) (Cui et al. 2019), and Parkinson's disease (Zhang et

86   al. 2019). In addition, Li et al. (Li et al. 2018a) discovered that in contrast to static ALFF

87   abnormalities, d-ALFF abnormalities could predict the severity of suicidal ideation in major

88   depressive disorders. d-ALFF may contribute more than ALFF in differentiating between

89   patients diagnosed with GAD and normal controls (Cui et al. 2019). However, as far as we know,

90   the dynamic signatures of ALFF have been rarely elucidated in ALS; furthermore, the

91   performance of d-ALFF compared with ALFF in recognizing ALS patients from healthy controls

92   (HCs) at an individual level remains poorly documented.

93   Motivated by previous studies, we utilized d-ALFF to detect changes of dynamic patterns of

94   brain activity in ALS. We assumed that patients with ALS would exhibit altered d-ALFF

95   patterns contrast to HCs, and that such changes could be used as features to distinguish them. We

96   also hypothesized that the classification performance with altered d-ALFF as features would be

97   comparable with that using altered static ALFF.

98 Materials & Methods

99 Subjects

100   In western countries, the rates of ALS is probably between 1 and 3 per 100 000 per year per

101   person-years (Robberecht & Philips 2013), while the exact prevalence in China remains unclear

102   (Chen et al. 2015). ALS is more widespread in men than in women in different countries (Chen

103   et al. 2015; Oskarsson et al. 2018). Patients were employed from January 1, 2009 to December

104   31, 2013 in this work. Fifty-four patients diagnosed with ALS and 54 HCs matched in gender

105   and age were enrolled from Southwest Hospital. The inclusion criteria were as follows: patients

106   can lie down flat in the scanner for at least 40 minutes and receive none therapeutic interventions

107   before participating in this study; and patients with ALS diagnosed on the basis of the revised El

108   Escorial criteria of the World Federation of Neurology (Brooks et al. 2000). The exclusion

109   criteria were as follows: patients diagnosed with frontotemporal dementia or other mental and

110   neurological disorders; patients with major systemic diseases; patients with family trait of motor

111   neuron diseases and other neurodegenerative disorders; and patients with cognitive impairment.

112   The clinical status based on ALS Functional Rating Scale-Revised (ALSFRS-R) was obtained

113   for each patient. Disease duration was computed from symptom onset to examination date. By

114   using the equation: (48-ALSFRS-R score)/Disease duration (Ellis et al. 1999), rate of disease

115   progression was achieved. Demographic and clinical information of subjects are displayed in

116   **Table 1.**

117   The measurements of the Edinburgh Handedness Inventory indicated that all the subjects

118   were right-handed. The medical research ethics committee of Southwest Hospital (the First

119   Affiliated Hospital of the Third Military Medical University of the Chinese People's Liberation

120   Army) authorized this study to proceed. Informed consent from each participant was collected.

121 Data acquisition

122   Data were collected as described in our former research (Ma et al. 2015). The following

123   parameters were used in collecting functional data: echo time (TE) = 30 ms, repetition time (TR)

124   = 2000 ms, flip angle (FA) = 90°, 36 slices, 1 mm gap, field of view (FOV) = 192 mm × 192

125   mm, thickness = 3 mm, matrix size = 64 × 64 and voxel size = 3 mm × 3 mm × 3 mm. Two

126   hundred and forty volumes were collected for each subject. T1-weighted structural data was

127   gathered using the following settings: TE = 2.52 ms, TR =1900 ms, FA = 9°, slice thickness = 1

128   mm, 176 slices, 0 mm gap, FOV = 256 mm × 256 mm, matrix size = 256 × 256, and voxel size =

129   1 mm × 1 mm × 1 mm.

130   **Data analysis**

131   **Preprocessing**

132   fMRI data preprocessing was performed with the Data Processing Assistant for Resting-

133   state fMRI (DPARSF) (Yan & Zang 2010). To ensure the reliabilty of functional data, we

134   abandoned the first 10 volumes of images. Slice timing and head motion have been done in the

135   remaining 230 volumes of images. No subject had a head movement bigger than 1.5 mm or

136   rotation bigger than 1.5°. The images were then normalized to the standard echo planar imaging

137   (EPI) template (resampled voxel size: 3 mm × 3 mm × 3 mm). The following images were

138   smoothed (full-width at half-maximum Gaussian kernel: 4 mm). After normalization, the time

139   series was linearly detrended. Except global signal, 24 parameters of head motion (Friston et al.

140   1996), signals of white matter, and signals of cerebrospinal fluid were all removed. ALFF/d-

141   ALFF was based on the frequency spectrum of rs-fMRI signals.

142   Total gray matter (GM) was obtained with the VBM8 toolbox as elaborated in the earlier

143   work (Ma et al. 2016; Ma et al. 2015).

144   **Static ALFF computation**

145   ALFF was calculated using DPARSF toolkit as used in prior research (Cheng et al. 2019;

146   Luo et al. 2012). With the aid of fast Fourier transform, the time series was transformed from the

147   time domain to a frequency domain, from which the power spectrum was achieved. With the

148   power spectrum of each voxel from all subjects, the square root was collected at each frequency

149   and then averaged in the region of 0.01–0.08 Hz (Guo et al. 2013). The square root obtained was

150   known as the ALFF at the given voxel. We divided the ALFF by the global mean ALFF for

151   standardization.

152   **d-ALFF computation**

153   d-ALFF was processed with Temporal Dynamic Analysis (TDA) toolkit which was

154   dependent on DPABI (Yan et al. 2016). According to a former report (Sakoglu et al. 2010), the

155   window length was supposed to be sufficiently short to capture transient signals and long enough

156   to detect slow changing signals. A sliding window with moderate size of 32 TR and a moving

157   step length of 1 TR were selected in this study (Chen et al. 2019b). The 230 time points were

158   divided into 199 windows. ALFF value was computed within each moving window for all

159   participants. Then, the standard deviation (SD) of all ALFF maps from moving windows was

160   computed to evaluate the variability of ALFF. Here, SD was used as d-ALFF.

161   **Statistical analysis**

162   Statistical analyses were processed with SPM12 toolkit. To compare differences in ALFF

163   and d-ALFF of two groups, we employed two-sample t-tests method. The factors such as age,

164   total GM volume, and gender were regressed. Gaussian Random Field (GRF) approach was

165   adopted to perform multiple comparisons. The voxel level and the cluster level was set $p < 0.01$

166   and $p < 0.05$ respectively (the minimum cluster size in ALFF and d-ALFF analyses was 78

167   voxels) in the GRF correction.

168   **Correlation analysis**

169   Based on region of interest (ROI), Pearson's correlation was analyzed to probe the relation

170   of alterations in ALFF/d-ALFF to the clinical data of ALS. The mean ALFF/d-ALFF value of

171   each significant clusters (ROIs) was used. A residual term was employed to correlate with

172   clinical data. Meanwhile, the total GM volume, age, and gender were regressed. Bonferroni

173   correction was introduced (significant level: $p < 0.05 / N$) in the present study. Here, $N = 15/12$

174   represented the amount of comparisons using ALFF and d-ALFF.

175   **Classification analysis**

176   Support vector machine (SVM) method was utilized to compare classification ability among

177   static ALFF, d-ALFF, and their combination for patients/HCs. The mean ALFF and d-ALFF of

178   each static ALFF's ROIs and d-ALFF's ROIs were used as classification features. Liblinear

179   toolbox with default parameter was utilized. Given that we aimed to compare the classification

180   ability among ALFF, d-ALFF, and their combination, a leave-one-out cross validation (LOOCV)

181   was accepted. LOOCV could obtain stable performance and prevent the possibility of overfitting

182   (Chen et al. 2019a; Liu et al. 2015). There were m (m = 108) LOOCV loops. In each loop, we

183   choose one participants' information to test the categorization model and the m - 1 participants'

184 information was selected for model training. Finally, specificity, sensitivity and accuracy were

185 collected to evaluate classifier performance.

186 **Validation analysis**

187 In order to confirm the main findings of d-ALFF, d-ALFF data with window lengths of 40

188 TRs and 50 TRs was recollected.

189 # Results

190 **Differences in static ALFF**

191 The ALFF in the ALS group increased in the right inferior temporal gyrus, right medial

192 superior frontal gyrus, and right medial superior frontal gyrus and reduced in the left middle

193 occipital gyrus and left precentral gyrus. The details were available in **Table 2** and **Figure 1a**.

194 **Differences in d-ALFF**

195 As shown in **Table 3** and **Figure 1b**, d-ALFF did not increase in ALS group. Decreased d-

196 ALFF was seen in the right lingual gyrus, left superior temporal gyrus, bilateral precentral gyrus,

197 and left paracentral lobule.

198 **Correlation analysis**

199 No correlation was detected between ALFF and clinical data in ALS. However, as shown in

200 **Figure 2**, the ALFF in the left superior orbitofrontal gyrus had a negative correlation with

201 ALSFRS-R score at a trend level ($p = 0.0096$, r = -0.3495, uncorrected). The ALFF in the left

202 superior orbitofrontal gyrus demonstrated a tendency of positive correlation with disease

203 progression rate (**Figure 3**, $p = 0.0135$, r = 0.3344, uncorrected). In addition, no significant

204 difference between d-ALFF and clinical data was found.

205 **Performance of classification**

206 **Figure 4** shows the receiver operating characteristic curve (ROC) with ALFF, d-ALFF, and

207 their combination. The numerical data of the area under the curve (AUC) with ALFF, d-ALFF,

208 and their combination were 0.82, 0.82 and 0.84 respectively.

209 As shown in **Table 4**, the ALFF method showed a classification accuracy of 76.85%, a

210 specificity of 72.22%, and a sensitivity of 81.48%. The d-ALFF index exhibited a classification

211 accuracy of 76.85%, a specificity of 62.96%, and a sensitivity of 90.74%. The accuracy,

212 specificity, and sensitivity of the combined ALFF and d-ALFF were 79.63%, 72.22%, and

213 87.04%, respectively.

214 **Validation results**

215   The results of d-ALFF using window sizes of 40 TRs and 50 TRs were very similar to the

216   major results of 32 TRs. Validation results were available in Supplementary Materials (**Fig. S1a**

217   and **Fig. S1b**).

Discussion

219   The present research studied the dynamic brain activity in ALS by using d-ALFF for the

220   first time. We found that: (1) patients with ALS showed decreased d-ALFF in the right lingual

221   gyrus, left superior temporal gyrus, bilateral precentral gyrus, and left paracentral lobule at

222   resting state, and (2) the combined ALFF and d-ALFF distinguished ALS from HCs with higher

223   accuracy than ALFF or d-ALFF alone.

Alterations in static ALFF

225   The brain areas with static ALFF differences in patients with ALS are consistent with

226   previous reports (Luo et al. 2012; Ma et al. 2016), except that the right inferior temporal gyrus

227   had increased ALFF. The temporal lobe with aberrant activation and connection in patients with

228   ALS was discovered in preceding rs-fMRI articles (Li et al. 2018b; Loewe et al. 2017; Zhou et

229   al. 2016). Besides, the thinning of cerebral cortex in the right inferior temporal gyrus is related to

230   rapid clinical progression in ALS (Verstraete et al. 2012). The right inferior temporal gyrus is

231   generally thought to be associated with social information processing for objects, places, and

232   faces (Grill-Spector 2003; Hall et al. 2005). Of note, the cognitive impairment of ALS includes

233   deficits in social cognition and executive functions (Beeldman et al. 2016). Moreover, deficits in

234   recognition of facial expressions of emotion in ALS have been documented (Zimmerman et al.

235   2007). However, the change in the ALFF value was not found in previous research on ALS (Luo

236   et al. 2012). The finding was probably caused by the situation that patients from the two studies

237   were at different stages of the disease. The previous study recruited patients with an earlier stage

238   compared with that in the present study, where the amplitude feature in this area may not altered.

239   However, more longitudinal research is need to make the result clear. Therefore, this functional

240   alteration may be the imaging evidence for understanding the impaired recognition of emotional

241   stimuli in ALS at a certain stage. Elevated ALFF in the left superior orbitofrontal gyrus was

242   relevant to rate of disease progression and ALSFRS-R score at a trend level. Hence, increased

243   ALFF in this area might be useful to understand the progress of ALS.

Alterations in d-ALFF

245   Compared with HCs, the d-ALFF in the right lingual gyrus was lower in ALS group.

246   Dysfunction of the right lingual gyrus in ALS was documented, including metabolic difference

247   (Verma et al. 2013) and functional connectivity (Li et al. 2018b). The lingual gyrus is an

248   important area in the visual system (Yang et al. 2015), and 24.13% of Chinese ALS population

249   are considered with visuospatial disability (Wei et al. 2015). Thus, we concluded that impairment

250   in the right lingual gyrus over time might underlie the phenomenon of visual dysfunction in

251   ALS.

252   This study also found reduced d-ALFF in the left superior temporal gyrus in ALS group.

253   The abnormality in left superior temporal gyrus was same with previous fMRI studies in regional

254   functional connectivity density (Li et al. 2018b) and with anatomical MRI studies in gray matter

255   volume (Buhour et al. 2017; Kim et al. 2017; Sheng et al. 2015). Electroencephalography study

256   (McMackin et al. 2019) shows decreased power in the left superior temporal gyrus when patients

257   with ALS underwent auditory frequency-mismatch oddball paradigm. The left superior temporal

258   gyrus was considered to be related to the function of auditory working memory (Leff et al.

259   2009). The quieter activity in the left superior temporal gyrus over time at resting state in ALS

260   can be explained as the reason of memory decline in ALS.

261   We also observed decreased d-ALFF in the bilateral precentral gyrus and left paracentral

262   lobule in ALS. These motor regions are hallmark areas for patients with ALS who had structural

263   (Cosottini et al. 2012; Schmidt et al. 2014; Thorns et al. 2013) and functional (Ma et al. 2016;

264   Zhang et al. 2017; Zhou et al. 2014) abnormalities. These motor regions were detected with static

265   ALFF and d-ALFF indices in the current research, indicating the vital role of these regions in

266   studying ALS.

267   **Relationship between static ALFF and d-ALFF changes**

268   d-ALFF and ALFF detected decreased activity in the precentral gyrus in patients suffering

269   from ALS. These findings provide a helpful perspective for our understanding the motor neuron

270   dysfunction of this disease. In addition, d-ALFF could provide other different changes compared

271   with traditional ALFF method, showing that dynamic brain activity may be an important

272   neuroimaging feature to track pathological changes in ALS.

273   Altered d-ALFF could identify patients with ALS from HCs, and the classification

274   performance is similar to that of ALFF. However, when both static and dynamic ALFF features

275   were combined, the classification performance achieved the highest overall accuracy rate. These

276 results consolidated that ALFF and d-ALFF were different approaches used to characterize brain

277 activity from different perspectives. In contrast to ALFF, d-ALFF could provide complementary

278 information to understand ALS better. The findings also provided a novel way to help

279 distinguish patients with ALS from the healthy population.

280 **Limitations and further considerations**

281 Several limitations should be noted in this work. First, the features in classification were

282 based on prior knowledge, which may increase the overall accuracy rate. The combined ALFF

283 and d-ALFF approach would enhance accuracy with a single feature. More subjects and further

284 sub-group analysis should be considered to obtain stable and more precise results.

285 ## Conclusions

286 ALFF and d-ALFF patterns were altered in patients with ALS. The alterations in the two

287 features could identify ALS at the individual level with nearly the same performance. However,

288 when the two features were combined, the classification performance achieved the highest

289 overall accuracy rate. These results provide evidence for applying dynamic spontaneous neural

290 activity (d-ALFF) to uncover the neuropathology of ALS.

291 ## Acknowledgments

292 The research was supported by the Cangzhou Science and Technology Research and

293 Development project (No. 162302137) and China Postdoctoral Science Foundation Grant (No.

294 2019M653383).

295 ## References

296 Abidi M, de Marco G, Couillandre A, Feron M, Mseddi E, Termoz N, Querin G, Pradat PF, and
297 Bede P. 2020. Adaptive functional reorganization in amyotrophic lateral sclerosis: coexisting
298 degenerative and compensatory changes. *European Journal of Neurology* 27:121-128.
299 Allen EA, Damaraju E, Plis SM, Erhardt EB, Eichele T, and Calhoun VD. 2014. Tracking whole-
300 brain connectivity dynamics in the resting state. *Cereb Cortex* 24:663-676.
301 Beeldman E, Raaphorst J, Klein Twennaar M, de Visser M, Schmand BA, and de Haan RJ. 2016.
302 The cognitive profile of ALS: a systematic review and meta-analysis update. *J Neurol Neurosurg*
303 *Psychiatry* 87:611-619. 10.1136/jnnp-2015-310734
304 Biswal B, Zerrin Yetkin F, Haughton VM, and Hyde JS. 1995. Functional connectivity in the
305 motor cortex of resting human brain using echo‐planar MRI. *Magnetic resonance in medicine*
306 34:537-541.
307 Bourke SC, Tomlinson M, Williams TL, Bullock RE, Shaw PJ, and Gibson GJ. 2006. Effects of
308 non-invasive ventilation on survival and quality of life in patients with amyotrophic lateral
309 sclerosis: a randomised controlled trial. *The Lancet Neurology* 5:140-147.
310 https://doi.org/10.1016/S1474-4422(05)70326-4

311   Brooks B, Miller RG, Swash M, and Munsat TL. 2000. *World Federation of Neurology Research*
312   *Group on Motor Neuron Diseases. El Escorial revisited: Revised criteria for the diagnosis of*
313   *amyotrophic lateral sclerosis.*
314   Bueno APA, Pinaya WHL, Rebello K, de Souza LC, Hornberger M, and Sato JR. 2019. Regional
315   dynamics of the resting brain in amyotrophic lateral sclerosis using fractional amplitude of low-
316   frequency fluctuations and regional homogeneity analyses. *Brain connectivity* 9:356-364.
317   Buhour M-S, Doidy F, Laisney M, Pitel AL, de La Sayette V, Viader F, Eustache F, and
318   Desgranges B. 2017. Pathophysiology of the behavioral variant of frontotemporal lobar
319   degeneration: A study combining MRI and FDG-PET. *Brain imaging and behavior* 11:240-252.
320   10.1007/s11682-016-9521-x
321   Chen H, Uddin LQ, Guo X, Wang J, Wang R, Wang X, Duan X, and Chen H. 2019a. Parsing
322   brain structural heterogeneity in males with autism spectrum disorder reveals distinct clinical
323   subtypes. *Hum Brain Mapp* 40:628-637. 10.1002/hbm.24400
324   Chen J, Sun D, Shi Y, Jin W, Wang Y, Xi Q, and Ren C. 2019b. Dynamic Alterations in
325   Spontaneous Neural Activity in Multiple Brain Networks in Subacute Stroke Patients: A Resting-
326   State fMRI Study. *Frontiers in neuroscience* 12:994-994. 10.3389/fnins.2018.00994
327   Chen L, Zhang B, Chen R, Tang L, Liu R, Yang Y, Yang Y, Liu X, Ye S, Zhan S, and Fan D.
328   2015. Natural history and clinical features of sporadic amyotrophic lateral sclerosis in China.
329   *Journal of Neurology, Neurosurgery, and Psychiatry* 86. 10.1136/jnnp-2015-310471
330   Cheng C, Dong D, Jiang Y, Ming Q, Zhong X, Sun X, Xiong G, Gao Y, and Yao S. 2019. State-
331   Related Alterations of Spontaneous Neural Activity in Current and Remitted Depression
332   Revealed by Resting-State fMRI. *Front Psychol* 10. 10.3389/fpsyg.2019.00245
333   Chipika RH, Finegan E, Shing SLH, Hardiman O, and Bede P. 2019. Tracking a fast-moving
334   disease: longitudinal markers, monitoring, and clinical trial endpoints in ALS. *Frontiers in*
335   *neurology* 10.
336   Cosottini M, Pesaresi I, Piazza S, Diciotti S, Cecchi P, Fabbri S, Carlesi C, Mascalchi M, and
337   Siciliano G. 2012. Structural and functional evaluation of cortical motor areas in Amyotrophic
338   Lateral Sclerosis. *Experimental Neurology* 234:169-180.
339   https://doi.org/10.1016/j.expneurol.2011.12.024
340   Cui Q, Sheng W, Chen Y, Pang Y, Lu F, Tang Q, Han S, Shen Q, Wang Y, and Xie A. 2019.
341   Dynamic changes of amplitude of low‐frequency fluctuations in patients with generalized
342   anxiety disorder. *Human brain mapping*.
343   Ellis C, Simmons A, Jones D, Bland J, Dawson J, Horsfield M, Williams S, and Leigh P. 1999.
344   *Diffusion tensor MRI assesses corticospinal tract damages in ALS.*
345   Friston KJ, Williams S, Howard R, Frackowiak RS, and Turner R. 1996. Movement-related
346   effects in fMRI time-series. *Magn Reson Med* 35:346-355.
347   Fu Z, Tu Y, Di X, Biswal BB, Calhoun VD, and Zhang Z. 2017. Associations between functional
348   connectivity dynamics and BOLD dynamics are heterogeneous across brain networks. *Frontiers*
349   *in human neuroscience* 11:593.
350   Grill-Spector K. 2003. The neural basis of object perception. *Curr Opin Neurobiol* 13:159-166.
351   Guo W-b, Liu F, Xue Z-m, Xu X-j, Wu R-r, Ma C-q, Wooderson SC, Tan C-l, Sun X-l, and Chen
352   J-d. 2012. Alterations of the amplitude of low-frequency fluctuations in treatment-resistant and
353   treatment-response depression: a resting-state fMRI study. *Progress in Neuro-*
354   *Psychopharmacology and Biological Psychiatry* 37:153-160.
355   Guo W, Liu F, Dai Y, Jiang M, Zhang J, Yu L, Long L, Chen H, Gao Q, and Xiao C. 2013.
356   Decreased interhemispheric resting-state functional connectivity in first-episode, drug-naive
357   major depressive disorder. *Progress in Neuro-Psychopharmacology and Biological Psychiatry*
358   41:24-29.
359   Hall DA, Fussell C, and Summerfield AQ. 2005. Reading fluent speech from talking faces:
360   typical brain networks and individual differences. *J Cogn Neurosci* 17:939-953.
361   10.1162/0898929054021175

362 Hardiman O, Al-Chalabi A, Chio A, Corr EM, Logroscino G, Robberecht W, Shaw PJ, Simmons
363 Z, and van den Berg LH. 2017. Amyotrophic lateral sclerosis. *Nature Reviews Disease Primers*
364 3:17071. 10.1038/nrdp.2017.71
365 Huynh W, Simon NG, Grosskreutz J, Turner MR, Vucic S, and Kiernan MC. 2016. Assessment
366 of the upper motor neuron in amyotrophic lateral sclerosis. *Clinical Neurophysiology* 127:2643-
367 2660. https://doi.org/10.1016/j.clinph.2016.04.025
368 Kawagoe T, Onoda K, and Yamaguchi S. 2019. Subjective memory complaints are associated
369 with altered resting-state functional connectivity but not structural atrophy. *NeuroImage: Clinical*
370 21:101675. https://doi.org/10.1016/j.nicl.2019.101675
371 Kim H-J, de Leon M, Wang X, Kim HY, Lee Y-J, Kim Y-H, and Kim SH. 2017. Relationship
372 between Clinical Parameters and Brain Structure in Sporadic Amyotrophic Lateral Sclerosis
373 Patients According to Onset Type: A Voxel-Based Morphometric Study. *PLOS ONE*
374 12:e0168424. 10.1371/journal.pone.0168424
375 Leff AP, Price CJ, Seghier ML, Schofield TM, Grogan A, Crinion JT, and Green DW. 2009. The
376 left superior temporal gyrus is a shared substrate for auditory short-term memory and speech
377 comprehension: evidence from 210 patients with stroke. *Brain* 132:3401-3410.
378 10.1093/brain/awp273
379 Li J, Duan X, Cui Q, Chen H, and Liao W. 2018a. More than just statics: temporal dynamics of
380 intrinsic brain activity predicts the suicidal ideation in depressed patients. *Psychological*
381 *Medicine*:1-9. 10.1017/S0033291718001502
382 Li W, Zhang J, Zhou C, Hou W, Hu J, Feng H, and Zheng X. 2018b. Abnormal Functional
383 Connectivity Density in Amyotrophic Lateral Sclerosis. *Front Aging Neurosci* 10:215.
384 10.3389/fnagi.2018.00215
385 Liao W, Li J, Ji G-J, Wu G-R, Long Z, Xu Q, Duan X, Cui Q, Biswal BB, and Chen H. 2019.
386 Endless fluctuations: temporal dynamics of the amplitude of low frequency fluctuations. *IEEE*
387 *transactions on medical imaging* 38:2523-2532.
388 Liu F, Guo W, Fouche J-P, Wang Y, Wang W, Ding J, Zeng L, Qiu C, Gong Q, Zhang W, and
389 Chen H. 2015. Multivariate classification of social anxiety disorder using whole brain functional
390 connectivity. *Brain Structure and Function* 220:101-115. 10.1007/s00429-013-0641-4
391 Liu F, Guo W, Liu L, Long Z, Ma C, Xue Z, Wang Y, Li J, Hu M, and Zhang J. 2013. Abnormal
392 amplitude low-frequency oscillations in medication-naive, first-episode patients with major
393 depressive disorder: a resting-state fMRI study. *Journal of affective disorders* 146:401-406.
394 Liu F, Wang Y, Li M, Wang W, Li R, Zhang Z, Lu G, and Chen H. 2017. Dynamic functional
395 network connectivity in idiopathic generalized epilepsy with generalized tonic–clonic seizure.
396 *Human brain mapping* 38:957-973. 10.1002/hbm.23430
397 Loewe K, Machts J, Kaufmann J, Petri S, Heinze HJ, Borgelt C, Harris JA, Vielhaber S, and
398 Schoenfeld MA. 2017. Widespread temporo-occipital lobe dysfunction in amyotrophic lateral
399 sclerosis. *Sci Rep* 7:40252. 10.1038/srep40252
400 Luo C, Chen Q, Huang R, Chen X, Chen K, Huang X, Tang H, Gong Q, and Shang H. 2012.
401 *Patterns of Spontaneous Brain Activity in Amyotrophic Lateral Sclerosis: A Resting-State fMRI*
402 *Study*.
403 Ma X, Zhang J, Zhang Y, Chen H, Li R, Long Z, Zheng J, Wang J, and Chen H. 2016.
404 Frequency-specific alterations in the fractional amplitude of low-frequency fluctuations in
405 amyotrophic lateral sclerosis. *Neurological Sciences*:1-9.
406 Ma X, Zhang J, Zhang Y, Chen H, Li R, Wang J, and Chen H. 2015. Altered cortical hubs in
407 functional brain networks in amyotrophic lateral sclerosis. *Neurological Sciences* 36:2097-2104.
408 10.1007/s10072-015-2319-6
409 McMackin R, Dukic S, Broderick M, Iyer PM, Pinto-Grau M, Mohr K, Chipika R, Coffey A,
410 Buxo T, Schuster C, Gavin B, Heverin M, Bede P, Pender N, Lalor EC, Muthuraman M,
411 Hardiman O, and Nasseroleslami B. 2019. Dysfunction of attention switching networks in

amyotrophic lateral sclerosis. *NeuroImage: Clinical* 22:101707.
https://doi.org/10.1016/j.nicl.2019.101707

Oskarsson B, Gendron TF, and Staff NP. 2018. Amyotrophic Lateral Sclerosis: An Update for 2018. *Mayo Clinic Proceedings* 93:1617-1628. https://doi.org/10.1016/j.mayocp.2018.04.007

Robberecht W, and Philips T. 2013. The changing scene of amyotrophic lateral sclerosis. *Nature Reviews Neuroscience* 14:248-264. 10.1038/nrn3430

Roth KA, and Shacka JJ. 2009. Apoptosis in Neurodegenerative Disease. In: Squire LR, ed. *Encyclopedia of Neuroscience*. Oxford: Academic Press, 531-537.

Sakoglu U, Pearlson GD, Kiehl KA, Wang YM, Michael AM, and Calhoun VD. 2010. A method for evaluating dynamic functional network connectivity and task-modulation: application to schizophrenia. *MAGMA* 23:351-366. 10.1007/s10334-010-0197-8

Schmidt R, Verstraete E, de Reus MA, Veldink JH, van den Berg LH, and van den Heuvel MP. 2014. Correlation between structural and functional connectivity impairment in amyotrophic lateral sclerosis. *Human Brain Mapping* 35:4386-4395. doi:10.1002/hbm.22481

Shen DC, Hou B, Cui B, Li XL, Peng P, Tai HF, Zhang K, Liu SW, Fu HH, Liu MS, Feng F, and Cui LY. 2018. [Resting-state functional MRI studies of amyotrophic lateral sclerosis patients with various levels of cognitive impairment]. *Zhonghua Yi Xue Za Zhi* 98:2002-2006. 10.3760/cma.j.issn.0376-2491.2018.25.007

Sheng L, Ma H, Zhong J, Shang H, Shi H, and Pan P. 2015. Motor and extra-motor gray matter atrophy in amyotrophic lateral sclerosis: quantitative meta-analyses of voxel-based morphometry studies. *Neurobiology of Aging* 36:3288-3299. https://doi.org/10.1016/j.neurobiolaging.2015.08.018

Sun Y, Dai Z, Li Y, Sheng C, Li H, Wang X, Chen X, He Y, and Han Y. 2016. Subjective cognitive decline: mapping functional and structural brain changes—a combined resting-state functional and structural MR imaging study. *Radiology* 281:185-192.

Thorns J, Jansma H, Peschel T, Grosskreutz J, Mohammadi B, Dengler R, and Münte TF. 2013. Extent of cortical involvement in amyotrophic lateral sclerosis – an analysis based on cortical thickness. *BMC Neurology* 13:148. 10.1186/1471-2377-13-148

Turner M, Kiernan MC, Leigh PN, and Talbot K. 2009. Biomarkers in amyotrophic lateral sclerosis. *Lancet Neurology* 8:94-109.

van Es MA, Hardiman O, Chio A, Al-Chalabi A, Pasterkamp RJ, Veldink JH, and van den Berg LH. 2017. Amyotrophic lateral sclerosis. *Lancet* 390:2084-2098. 10.1016/S0140-6736(17)31287-4

Verma G, Woo JH, Chawla S, Wang S, Sheriff S, Elman LB, McCluskey LF, Grossman M, Melhem ER, Maudsley AA, and Poptani H. 2013. Whole-brain analysis of amyotrophic lateral sclerosis by using echo-planar spectroscopic imaging. *Radiology* 267:851-857. 10.1148/radiol.13121148

Verstraete E, and Foerster BR. 2015. Neuroimaging as a new diagnostic modality in amyotrophic lateral sclerosis. *Neurotherapeutics* 12:403-416.

Verstraete E, Veldink JH, Hendrikse J, Schelhaas HJ, van den Heuvel MP, and van den Berg LH. 2012. Structural MRI reveals cortical thinning in amyotrophic lateral sclerosis. *Journal of Neurology, Neurosurgery & Psychiatry* 83:383-388. 10.1136/jnnp-2011-300909

Volanti P, Cibella F, Sarvà M, De Cicco D, Spanevello A, Mora G, and La Bella V. 2011. Predictors of non-invasive ventilation tolerance in amyotrophic lateral sclerosis. *Journal of the neurological sciences* 303:114-118.

Wei Q, Chen X, Zheng Z, Huang R, Guo X, Cao B, Bak TH, and Shang H. 2015. Screening for cognitive impairment in a Chinese ALS population. *Amyotrophic Lateral Sclerosis and Frontotemporal Degeneration* 16:40-45. 10.3109/21678421.2014.966311

Yan C-G, and Zang Y-F. 2010. *DPARSF: a MatLab toolbox for "pipeline" data analysis of resting-state fMRI.*

9000

462 Yan CG, Wang XD, Zuo XN, and Zang YF. 2016. DPABI: Data Processing & Analysis for
463 (Resting-State) Brain Imaging. *Neuroinformatics* 14:339-351. 10.1007/s12021-016-9299-4
464 Yang S, Meng Y, Li J, Fan Y-S, Du L, Chen H, and Liao W. 2019. Temporal dynamic changes of
465 intrinsic brain activity in schizophrenia with cigarette smoking. *Schizophrenia research* 210:66-
466 72.
467 Yang Y-L, Deng H-X, Xing G-Y, Xia X-L, and Li H-F. 2015. Brain functional network
468 connectivity based on a visual task: visual information processing-related brain regions are
469 significantly activated in the task state. *Neural regeneration research* 10:298-307. 10.4103/1673-
470 5374.152386
471 Yu-Feng Z, Yong H, Chao-Zhe Z, Qing-Jiu C, Man-Qiu S, Meng L, Li-Xia T, Tian-Zi J, and Yu-
472 Feng W. 2007. Altered baseline brain activity in children with ADHD revealed by resting-state
473 functional MRI. *Brain and Development* 29:83-91.
474 Zhang C, Dou B, Wang J, Xu K, Zhang H, Sami MU, Hu C, Tao R, Chen N, and Li K. 2019.
475 Dynamic Alterations of Spontaneous Neural Activity in Parkinson's Disease: A Resting-State
476 fMRI Study. *Frontiers in neurology* 10:1052.
477 Zhang J, Ji B, Hu J, Zhou C, Li L, Li Z, Huang X, and Hu X. 2017. Aberrant interhemispheric
478 homotopic functional and structural connectivity in amyotrophic lateral sclerosis. *J Neurol
479 Neurosurg Psychiatry* 88:369-370. 10.1136/jnnp-2016-314567
480 Zhou C, Hu X, Hu J, Liang M, Yin X, Chen L, Zhang J, and Wang J. 2016. Altered Brain
481 Network in Amyotrophic Lateral Sclerosis: A Resting Graph Theory-Based Network Study at
482 Voxel-Wise Level. *Frontiers in neuroscience* 10:204-204. 10.3389/fnins.2016.00204
483 Zhou F, Xu R, Dowd E, Zang Y, Gong H, and Wang Z. 2014. Alterations in regional functional
484 coherence within the sensory-motor network in amyotrophic lateral sclerosis. *Neuroscience
485 Letters* 558:192-196. https://doi.org/10.1016/j.neulet.2013.11.022
486 Zimmerman EK, Eslinger PJ, Simmons Z, and Barrett AM. 2007. Emotional perception deficits
487 in amyotrophic lateral sclerosis. *Cogn Behav Neurol* 20:79-82.
488 10.1097/WNN.0b013e31804c700b
489 Zou Q, Wu CW, Stein EA, Zang Y, and Yang Y. 2009. Static and dynamic characteristics of
490 cerebral blood flow during the resting state. *Neuroimage* 48:515-524.
491 https://doi.org/10.1016/j.neuroimage.2009.07.006
492

Figure 1

Results of ALFF and d-ALFF analyses by two-sample t-tests between ALS group and HC group.

a. Brain regions with significant difference in static ALFF between the ALS group and HC group. b. Brain regions with significant difference in d-ALFF between the ALS group and HC group. The voxel level was set at $p < 0.01$, and the cluster level was set at $p < 0.05$ with GRF corrected. The color bar represents the T value of the between-group analysis. Hot colors represent higher ALFF/d-ALFF in the ALS group than in the healthy control group, and cool colors represent the lower ALFF/d-ALFF in the ALS group than the healthy control group.
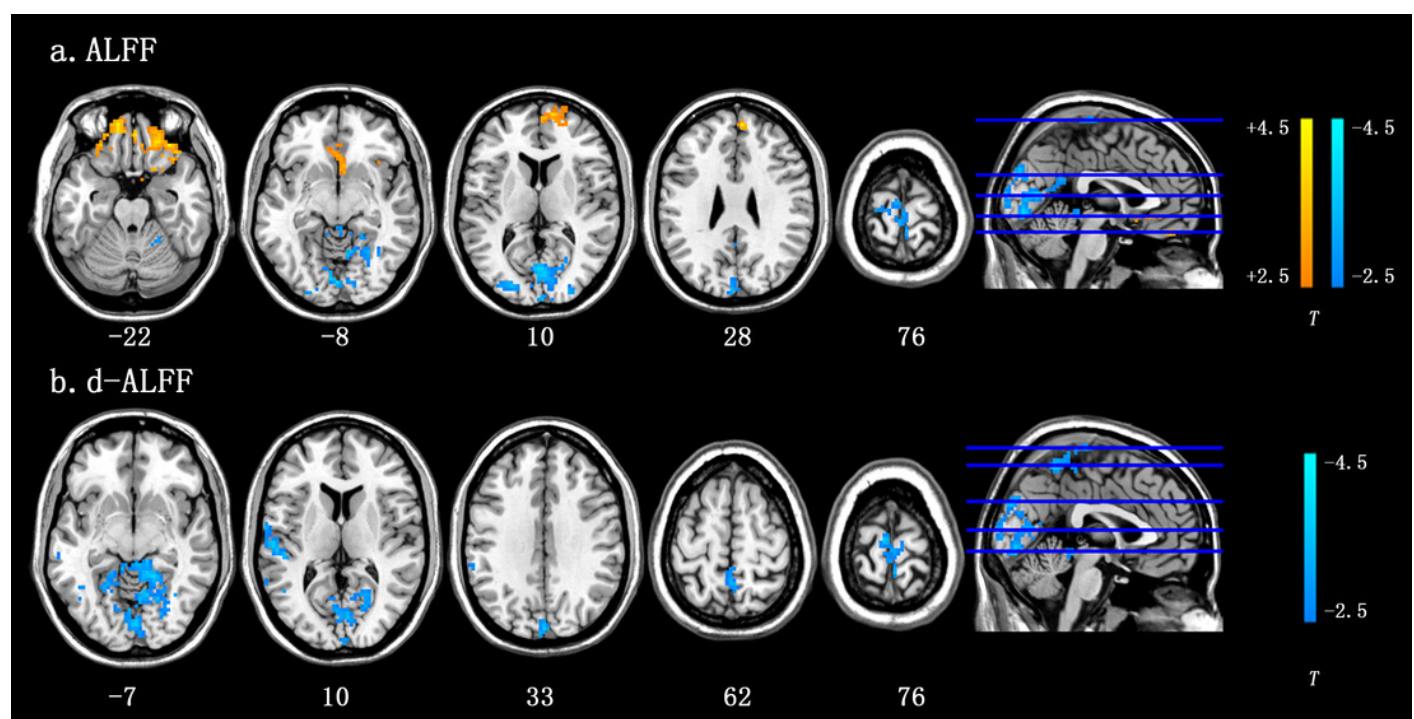
Figure 2

Correlation between ALFF value in the left superior orbitofrontal gyrus and ALSFRS-R score in the ALS group.

Correlation between ALFF value in the left superior orbitofrontal gyrus and ALSFRS-R score in the ALS group.
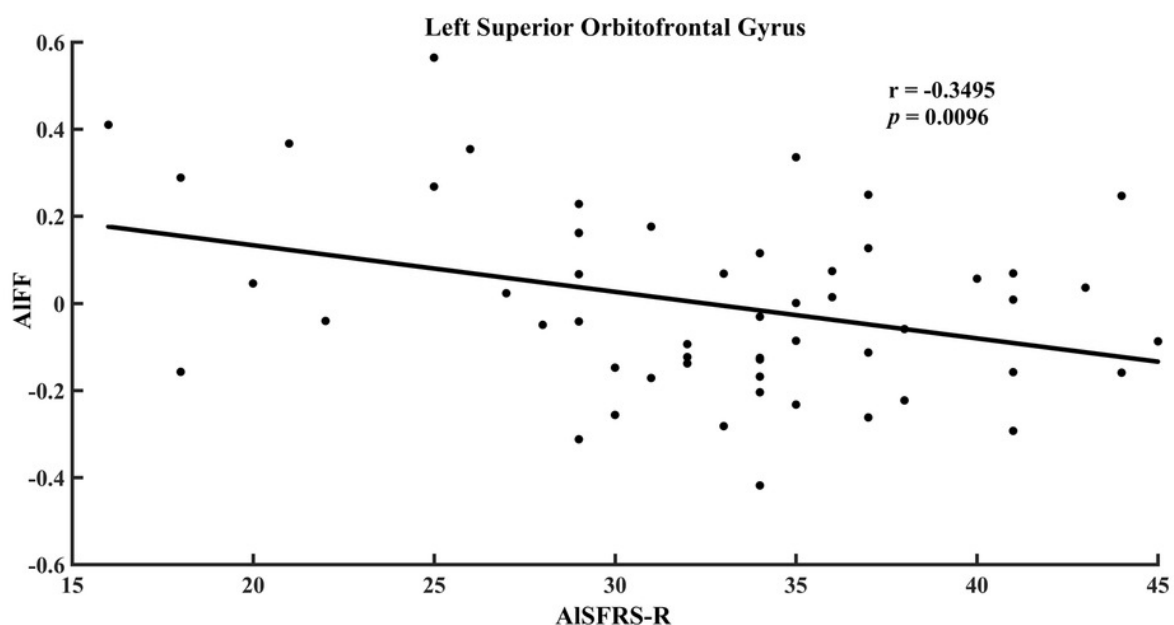
Figure 3

Correlation between ALFF value in the left superior orbitofrontal gyrus and disease progression rate in the ALS group.

Correlation between ALFF value in the left superior orbitofrontal gyrus and disease progression rate in the ALS group.
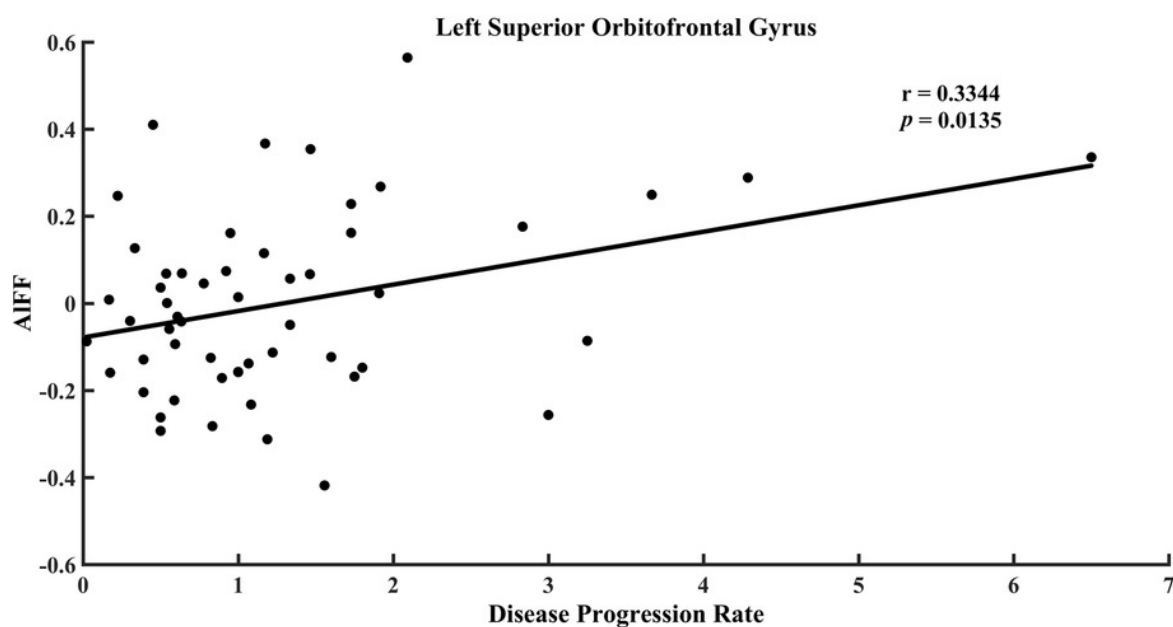
Figure 4

Receiver operating characteristic curve of the classifier with ALFF, d-ALFF, and their combination.

Receiver operating characteristic curve of the classifier with ALFF, d-ALFF, and their combination.
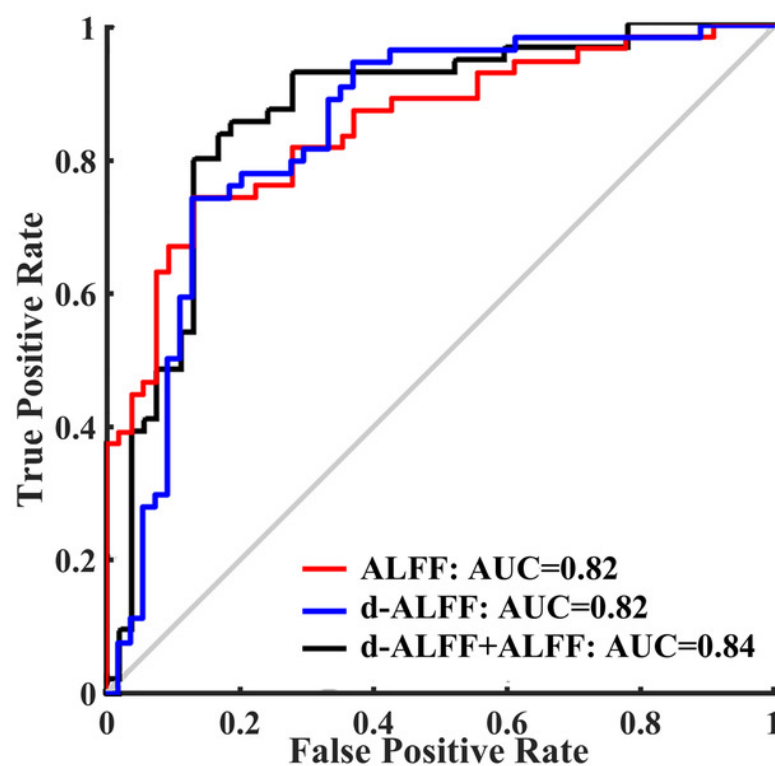
Demographic and clinical characteristics of the ALS patients and HCs.

Values are mean ± variance. ALS, Amyotrophic Lateral Sclerosis. HC, Healthy Control. ALSFRS-R, ALS Functional Rating Scale-revised. Disease progression rate, (48-ALSFRS-R score) / time from symptom onset. [a] The *p* value was obtained by Chi-square t-test. [b] The *p* value was obtained by two-sample t-test.

Table 1. Demographic and clinical characteristics of the ALS patients and HCs.

Variables	ALS (n = 54)	HC (n = 54)	*p* value
Gender (female/male)	18/36	18/36	1[a]
Age (years)	48.71 ±10.21	48.30 ± 8.74	0.82[b]
Gray matter	649.56 ±2842.17	668.23 ± 3251.82	0.08[b]
Disease duration (months)	20.93 ±21.56	—	—
ALSFRS-R	32.56 ± 6.83	—	—
Disease progression rate	1.28 ± 1.15	—	—

Values are mean ± variance. ALS, Amyotrophic Lateral Sclerosis. HC, Healthy Control. ALSFRS-R, ALS Functional Rating Scale-revised. Disease progression rate, (48-ALSFRS-R score) / time from symptom onset. [a] The *p* value was obtained by Chi-square t-test. [b] The *p* value was obtained by two-sample t-test.

Differences in ALFF between ALS and HC groups.

MNI, Montreal Neurological Institute. X, Y, Z, coordinates of primary peak locations in the MNI space. ALS, Amyotrophic Lateral Sclerosis. HC, Healthy Control. T value denotes the statistic value of two-sample t-test by contrasting the ALS patients to the controls ($p < 0.01$, GRF-corrected at a cluster level of $p < 0.05$).

1   **Table 2. Differences in ALFF between ALS and HC groups.**

Clusters	Brain regions	Cluster size (voxels)	MNI (X,Y,Z)	T value
ALS > HC				
Cluster 1	Right inferior temporal gyrus	128	45, -6, -45	4.14
Cluster 2	Left superior orbitofrontal gyrus	442	-15, 18, -15	4.45
Cluster 3	Right medial superior frontal gyrus	93	6, 54, 27	4.35
ALS < HC				
Cluster 1	Left middle occipital gyrus	895	-27, 90, -3	-4.56
Cluster 2	Left precentral gyrus	108	-27, -21, 72	-3.81

2   MNI, Montreal Neurological Institute. X, Y, Z, coordinates of primary peak locations in the MNI space. ALS,

3   Amyotrophic Lateral Sclerosis. HC, Healthy Control. T value denotes the statistic value of two-sample t-test by

4   contrasting the ALS patients to the controls ($p < 0.01$, GRF-corrected at a cluster level of $p < 0.05$).

Differences in d-ALFF between ALS and HC groups.

MNI, Montreal Neurological Institute. X, Y, Z, coordinates of primary peak locations in the MNI space. ALS, Amyotrophic Lateral Sclerosis. HC, Healthy Control. T value denotes the statistic value of two-sample t-test by contrasting the ALS patients to the controls ($p < 0.01$, GRF-corrected at a cluster level of $p < 0.05$).

1 **Table 3. Differences in d-ALFF between ALS and HC groups.**

Clusters	Brain regions	Cluster size (voxels)	MNI (X,Y,Z)	T value
ALS > HC				
None				
ALS < HC				
Cluster 1	Right lingual gyrus	988	24,-45, -9	-4.35
Cluster 2	Left superior temporal gyrus	176	-48,-27, 12	-3.82
Cluster 3	Bilateral precentral gyrus	90	51,-9, 24	-3.45
Cluster 4	Left paracentral lobule	125	-6, -15, 75	-3.70

2   MNI, Montreal Neurological Institute. X, Y, Z, coordinates of primary peak locations in the MNI space. ALS,

3   Amyotrophic Lateral Sclerosis. HC, Healthy Control. T value denotes the statistic value of two-sample t-test by

4   contrasting the ALS patients to the controls ($p < 0.01$, GRF-corrected at a cluster level of $p < 0.05$).

Performance evaluation of classifier using ALFF, d-ALFF and combined ALFF and d-ALFF.

1 **Table 4. Performance evaluation of classifier using ALFF, d-ALFF and combined ALFF and d-ALFF.**

	Sensitivity (%)	Specificity (%)	Accuracy (%)
ALFF	81.48	72.22	76.85
d-ALFF	90.74	62.96	76.85
combined ALFF and d-ALFF	87.04	72.22	79.63